Supplementary Information

Design of Proton-Conducting $Sn_{0.95}Al_{0.05}P_2O_7$ with Mesoporous Structure

Takashi Hibino[a,*], Kazuyo Kobayashi[a] and Satoru Fujita[b]

[a]Graduate School of Environmental Studies, Nagoya University, Nagoya 464-8601, Japan

[b]Toyota Central Research and Development Laboratories, Inc., Nagakute, Aichi 480-1192, Japan

Table of contents **Page**

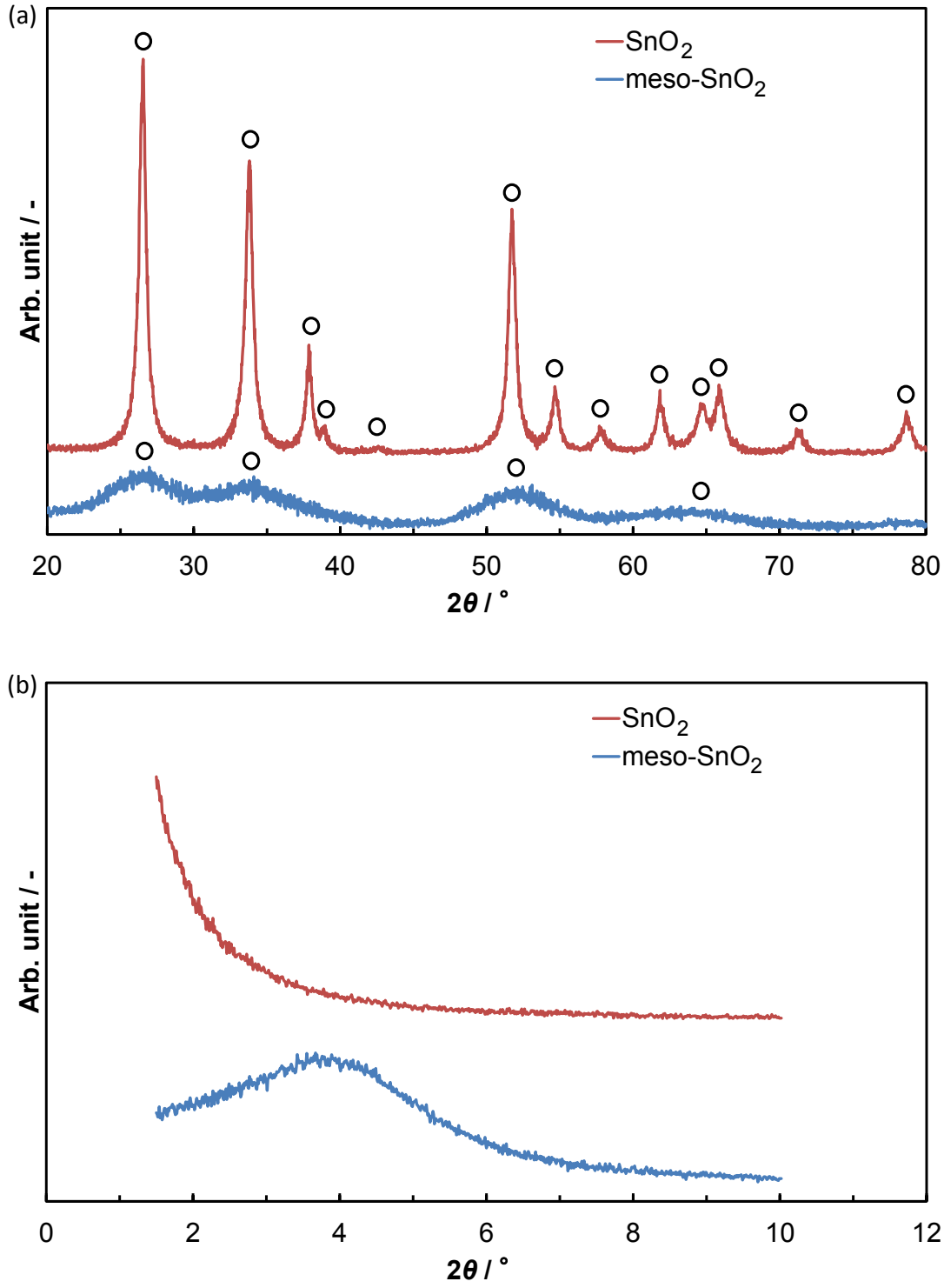

Fig. S1. XRD patterns for the mesoporous and nonporous SnO_2. (a) Data obtained in the Bragg angle range of 20-80° and (b) Data obtained in the Bragg angle range of 1.5-10°.

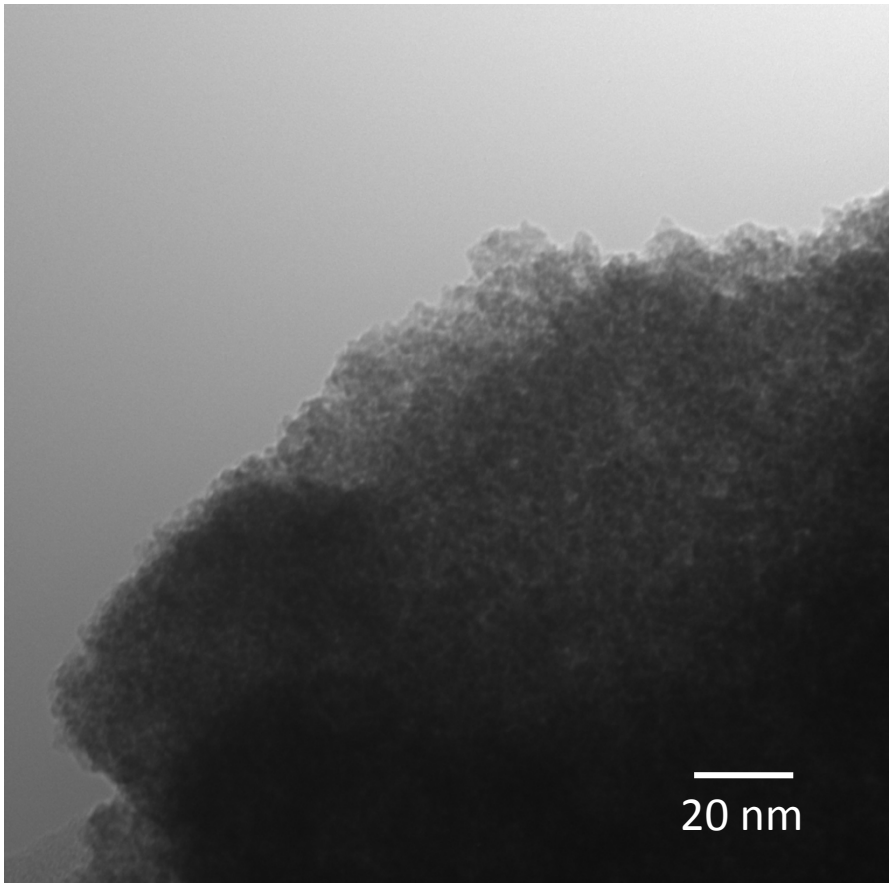

Fig. S2. TEM image of the mesoporous SnO_2.

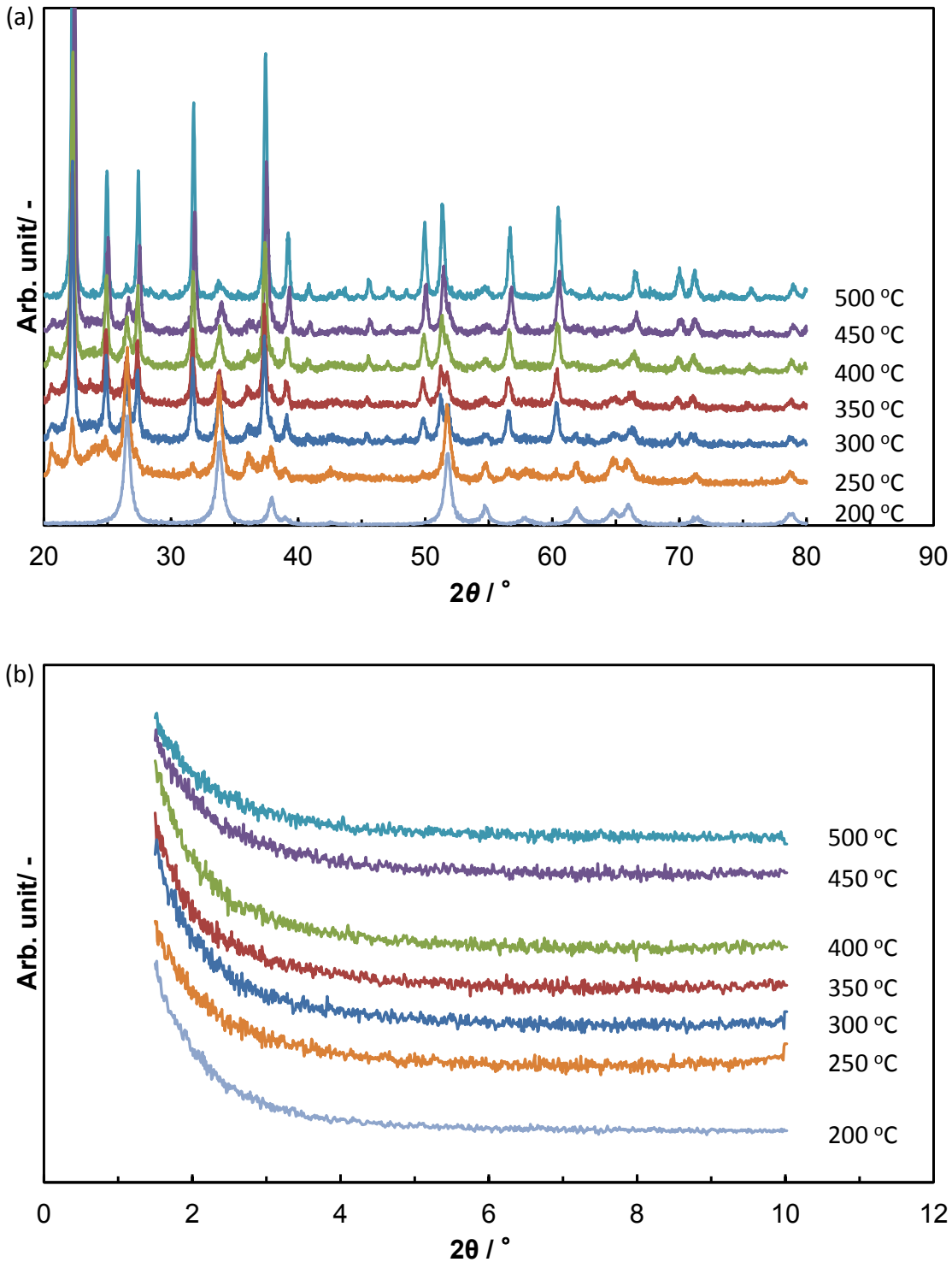

Fig. S3. XRD patterns for the SnP_2O_7 synthesized from a nonporous SnO_2 powder at various temperatures. (a) Data obtained in the Bragg angle range of 20-80° and (b) Data obtained in the Bragg angle range of 1.5-10°.

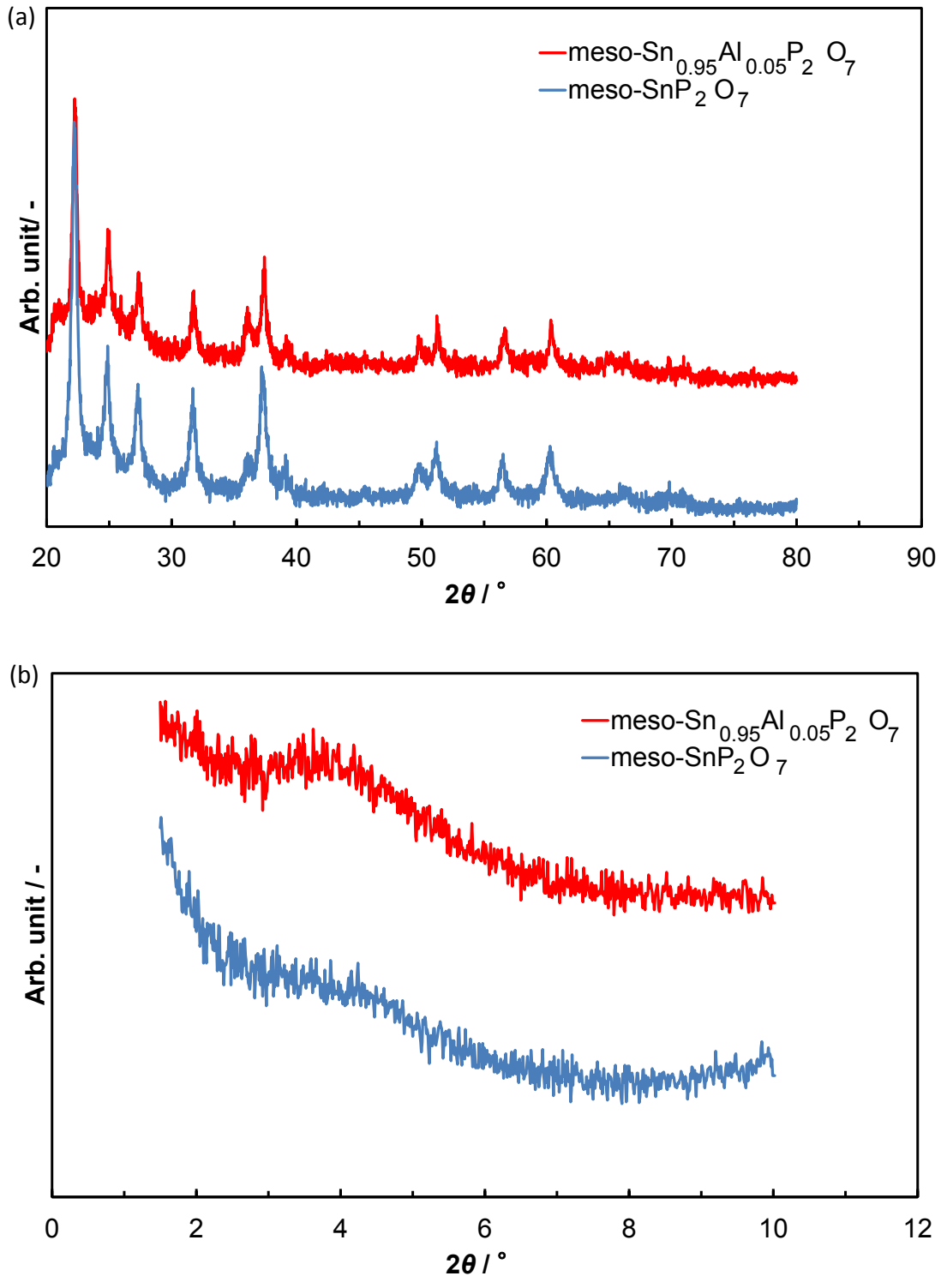

Fig. S4. XRD patterns for the mesoporous $Sn_{0.95}Al_{0.05}P_2O_7$ and SnP_2O_7. (a) Data obtained in the Bragg angle range of 20-80° and (b) Data obtained in the Bragg angle range of 1.5-10°.

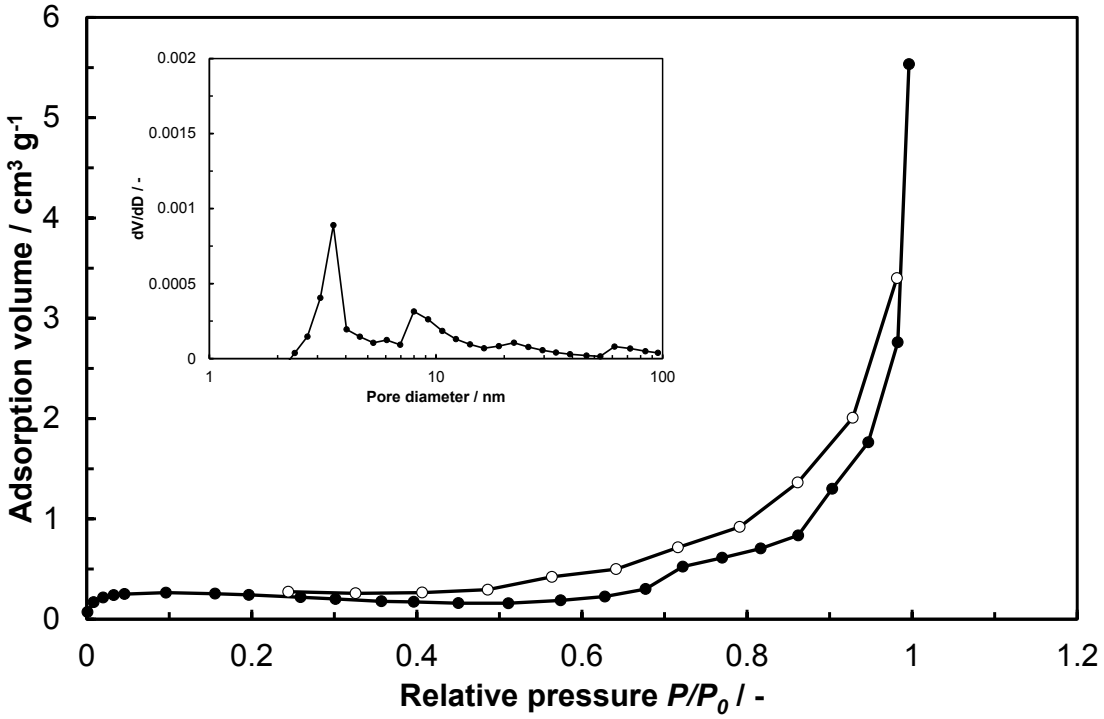

Fig. S5. Nitrogen gas adsorption/desorption isotherm for the $Sn_{0.95}Al_{0.05}P_2O_7$ sample synthesized from a mesoporous $Sn_{0.95}Al_{0.05}O_{1.975}$ powder at 250 °C. The inset is the pore distribution of the sample.

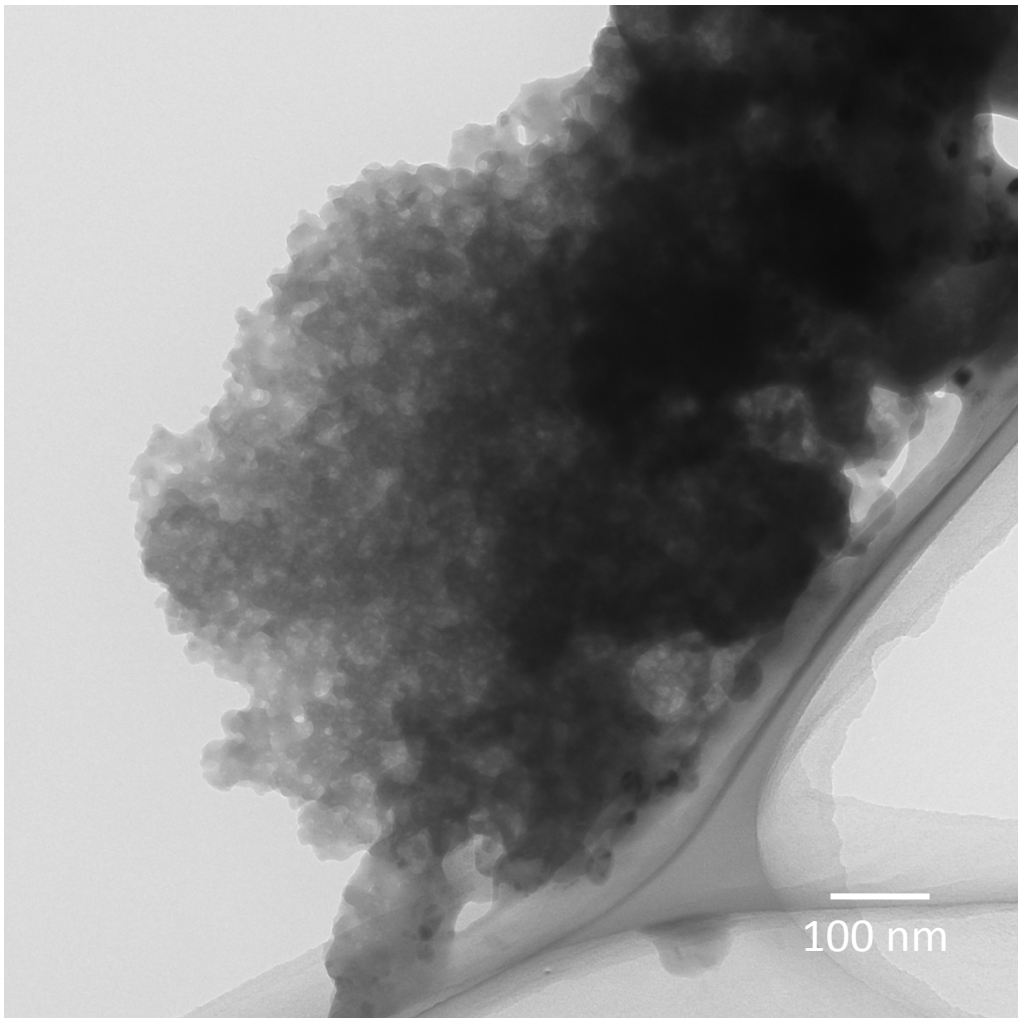

Fig. S6. TEM image of the SnP_2O_7 sample synthesized from a mesoporous $Sn_{0.95}Al_{0.05}O_{1.975}$ powder at 250 °C.